Regulating the Direction that Power Flows in Microwave Transmission Line Systems with Huygens Sources

Da Yi, Xing-Chang Wei, Ming-Chun Tang, and Richard W. Ziolkowski

***Abstract*—An innovative method based on Huygens sources to regulate the direction that power flows in microwave transmission line systems is developed and confirmed with measurements. The phase difference between the electric and magnetic currents in the Huygens source is utilized to finely control the ratio of the wave propagation amplitudes and, hence, power flows along the transmission line in opposite directions. The operating principles are elucidated with both the field distributions in a rectangular waveguide as the transmission line system and the voltages and currents in a transmission line circuit model driven by Huygens sources. The transmission line circuit models excited with electric and magnetic current sources separately and with their balanced combination provide a precise means to quantitatively demonstrate the tunability of the power flow with the Huygens source. A proof-of-concept experiment was implemented in a microwave rectangular waveguide to validate the theoretical analysis. The measured results, in good agreement with their simulated values, demonstrate that the reported approach leads to a wideband operation and large dynamic directional power ratios that are advantageous in the design of multifunctional electromagnetic devices and systems.**

***Index Terms*—Directional power flow, Huygens source, transmission lines**

I. Introduction

With the development of fifth-generation (5G) communication networks and Internet of Things (IoT) devices, multifunctional radio-frequency (RF) equipment and systems are in great demand. Their multiple functions are typically achieved by controlling the power flow in their circuits and structures. In general, there exist two approaches to control these power flows. The first employs digital switches to select the signal pathways in separate circuits or structures. This method has been widely used to realize reconfigurable filters [1], [2]; antennas [3], [4]; metasurfaces [5], [6]; and RF systems [7]. Unfortunately, this approach generally has poor space utilization because it requires large numbers of switches. The second method consists of inserting additional structures or materials into the circuits to control the signal power flow. For instance, coupling holes/slots [8], [9]; inductive walls [10]; ridge gap waveguide [11], [12]; epsilon-negative structures and branch line structures [14] have been implemented as directional couplers and power dividers to control the power pathways in circuits. Similarly, ferromagnetic materials have been used in circulators to regulate the power flow directions [15]. However, most of these elements are loaded into the signal's transmission pathway and thus lead to inescapable increases in loss, space requirements, complexities, and costs.

Huygens source antennas have been investigated and developed in recent years to control the far-field spatial distribution of radiated power. They utilize specific combinations of electric and magnetic dipoles/currents [16]-[26]. Many of these designs have focused on miniaturization [20]-[26], bandwidth enhancement [22], and reconfigurability [23], [25]. Huygens sources have also been developed to exhibit near-field directionality [27] and far-field needle radiation [28]; to achieve a nanoparticle laser [29]; to excite spin-momentum locking phenomena [30]-[32]; and to enable topological waveguides [33]. It is noted that while Huygens sources have found numerous implementations for antennas and quantum optics applications [16]-[33], few have been employed in microwave transmission line systems and devices. To the best of our knowledge, Huygens sources as the total-field/scattered-field boundaries used to launch waves numerically into the simulation regions treated with full-wave Maxwell equation solvers are the only ones applied to the understanding and design of waveguide systems [34]-[36].

In this Communication, Huygens sources are introduced into microwave transmission line systems. They act as the excitation sources of the transmission line system. More importantly, they are designed to arbitrarily control the amounts of power flowing along the transmission line in opposite directions. The phase difference between the electric and magnetic currents of the Huygens source is made tunable; and, as a consequence, their combination enables the ability to regulate the power flow. Notably, this feature expedites being able to fine tune the power ratio between the two directions. The approach is attractive because it facilitates the realization of multiple functions such as directional coupling and power dividing with a single simple circuit that has a small footprint and is low in cost. This concept is applied directly to a metallic rectangular waveguide system to illustrate its performance characteristics. Neither modifications of the overall waveguide shape nor the addition of structures in the signal's propagation pathway are necessary. Therefore, it holds promise to be an advanced building block for a series of new multifunctional integrated RF systems.

This Communication is organized as follows. First, a basic explanation of the Huygens source-based tunable power flow approach is introduced in a microwave rectangular waveguide transmission system in Section II. This Huygens source consists of a simple pair of ideal electric and magnetic currents. The operating principles are explained with the analytical field distributions. An equivalent transmission line model is also introduced to further quantify them. The Huygens source prototype and the experiments that were performed to validate the developed approach are described in Section III. The measured results clearly demonstrate that the advantages of the approach include a wide operating bandwidth, large-scale dynamic tunability, and multiple functionalities. Conclusions are discussed in Section IV. All of the simulated results reported herein were obtained with the ANSYS Electromagnetics Suite v. 19.2.

Manuscript received on 8th, November, 2019; revised on 30th, March, 2020; and accepted on 26th, May.

This work was supported in part by the National Natural Science Foundation of China contract number 61871467 and 61922018, in part by the Chongqing Natural Science Foundation contract number cstc2019jcyjjqX0004, and in part by the Australian Research Council grant number DP160102219. (*Corresponding author: Ming-Chun Tang.*)

D. Yi and M.-C. Tang are with the Key Laboratory of Dependable Service Computing in Cyber Physical Society Ministry of Education, College of Microelectronics and Communication Engineering, Chongqing University, Chongqing 400044, China, and also with Chongqing Key Laboratory of Space Information Network and Intelligent Information Fusion, Chongqing University, Chongqing, 400044, China. (e-mail: yida_cqu@cqu.edu.cn, tangmingchun@cqu.edu.cn)

X.-C. WEI is with College of Information Science and Electronic Engineering, Zhejiang University, No.38 Zheda Road, HangZhou 310027, China. (e-mail: weixc@zju.edu.cn).

R. W. Ziolkowski is with the Global Big Data Technologies Centre, University of Technology Sydney, Ultimo, NSW 2007, Australia. (e-mail: richard.ziolkowski@uts.edu.au).

II. The Proposed Method

A Huygens source consists of a properly balanced pair of in-phase electric and magnetic currents that are oriented orthogonal to each other. The placement of an idealized version of this oriented current pair in the center of a rectangular (WR-90) waveguide is illustrated in Fig. 1. An infinitesimal electric dipole is oriented along the x-axis with the electric current moment I_e; an infinitesimal magnetic dipole is oriented along the y-axis with the magnetic current moment I_m. Simulations of this configuration at 10 GHz indicate that if the magnitudes of their current moments satisfy the balanced condition $|I_e| = 1.75\ \eta_0\ |I_m|$, where η_0 is the wave impedance in free space, they produce the desired total cancellation of the fields radiated backwards from the source plane, i.e., into the $-z$ direction, and direct all of the radiated power broadside to the pair in the $+z$ direction.

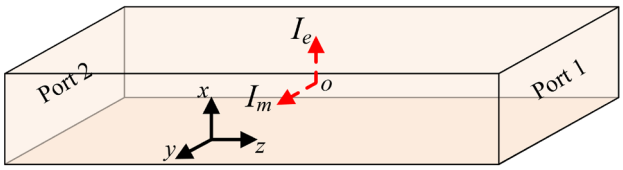

Fig. 1. The Huygens source model in a rectangular waveguide.

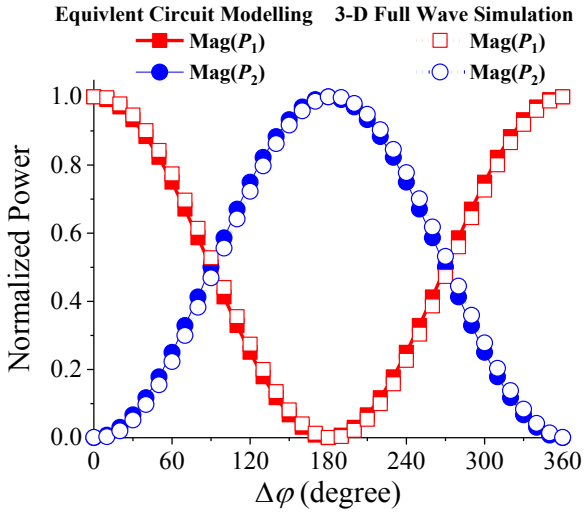

Fig. 2. The normalized powers received at the two ports with respect to the phase difference between the electric and magnetic currents.

The simulated normalized magnitudes of the power received at port 1 and at port 2 of the waveguide are shown in Fig. 2 as functions of the phase difference between I_e and I_m, i.e. $\Delta\varphi = \varphi_e - \varphi_m$. When the two dipoles are excited in-phase, i.e., $\Delta\varphi = 0°$, all of the radiated power flows to port 1. On the other hand, when they are excited completely out-of-phase, i.e., with $\Delta\varphi = 180°$ (current on one element is reversed from the in-phase case), all of the radiated power flows to port 2. These results clearly demonstrate the realization of unidirectional propagation in the transmission line system. Clearly, the value of $\Delta\varphi$ controls the ratio of the power flowing towards both ports. As shown in Fig. 2, very fine control of these powers and, hence, their ratio is possible. Note that when $\Delta\varphi = 90°$ or $270°$, the power specifically flows to both ports equally. Hence, this waveguide-Huygens source configuration acts as a natural 3-dB power divider, thus eliminating the need for both a source and a 3-dB waveguide power splitter.

The previous studies of Huygens sources [16]-[33] have mainly emphasized the cases when $\Delta\varphi = 0°$ and $180°$ to generate unidirectional propagation phenomena. Here, in contrast, the design is extended to realize an electromagnetic source that has the ability to regulate the directional flow of power in a microwave transmission system with high precision. The basic concept can be applied to any microwave transmission line system.

The unidirectional propagation, which occurs when $\Delta\varphi = 0°$ and $180°$, can be explained in terms of the representation of the TE modes generated by idealized electric and magnetic sources in an air-filled waveguide whose dimensions only allow propagation of the fundamental mode. Its spectral representation also immediately connects these propagating fields to an equivalent one-dimensional transmission line model. Let these sources lie in the plane $z = 0$. Let the size of the waveguide be a along the x-axis and b along the y-axis. The total fields of the fundamental propagating TE modes (TE_{01} mode in our coordinates) generated by the combination of an x-oriented electric source and a y-oriented magnetic source excited at the frequency $f = \omega/2\pi$ can be written in the form [8, Sec. 4.7]:

$$E_{\omega x}^{total} = E_{\omega x}^{elec} + E_{\omega x}^{mag} = \frac{1}{2}\left[A_e + Z_{TE}A_m\right]\sin\left(k_y y\right)e^{-jk_z z}\theta(z) + \frac{1}{2}\left[A_e - Z_{TE}A_m\right]\sin\left(k_y y\right)e^{+jk_z z}\theta(-z) \quad (1)$$

$$H_{\omega y}^{total} = H_{\omega y}^{elec} + H_{\omega y}^{mag} = \frac{1}{2}\left[\frac{A_e}{Z_{TE}} + A_m\right]\sin\left(k_y y\right)e^{-jk_z z}\theta(z) - \frac{1}{2}\left[\frac{A_e}{Z_{TE}} - A_m\right]\sin\left(k_y y\right)e^{+jk_z z}\theta(-z) \quad (2)$$

where the step function $\theta(z) = 1$ if $z > 0$ and $\theta(z) = 0$ if $z < 0$; $k_z = \sqrt{\omega^2\varepsilon_0\mu_0 - k_y^2}$; the transverse wavenumber $k_y = \pi/b$; and the wave impedance $Z_{TE} = \omega\mu_0/k_z$. The electric fields excited by the electric and magnetic current sources are, respectively, even- and odd-symmetric with respect to the location of the Huygens source combination. The ½ factor emphasizes that the sources, independently, radiate their power equally in the $\pm z$ directions. The amplitudes $A_{e,m} = |A_{e,m}|e^{j\varphi_{e,m}}$. It is then clear that the field amplitudes are balanced if $|A_e| = Z_{TE}|A_m|$, i.e., if they are in-phase with $\Delta\varphi = \varphi_e - \varphi_m = 0°$, the total electric and magnetic fields are zero for $z < 0$ and, hence, unidirectional in the $+z$-direction. It is then unidirectional in the $-z$-direction when they are $180°$ out of phase, i.e., $\Delta\varphi = 180°$. In our corresponding three-dimensional (3-D) full-wave simulation studies, the electric and magnetic currents radiate their spherical wave fields and they are quickly transformed into the corresponding TE_{01} modes because all other modes are evanescent. The amplitudes of those propagating modes follow from the spectral decomposition of their radiated fields into the waveguide modes. These 3-D simulations show that the magnitudes of the resulting fundamental modes are balanced if their source currents satisfy $|I_e| = 1.75\eta_0|I_m|$ at 10 GHz. This corresponds to the noted analytical balanced condition: $|A_e| = Z_{TE}|A_m|$.

The transmission line representation of the Huygens phenomenon in the waveguide is illustrated in Fig. 3. The two segments of the waveguide in the two opposite directions from the source plane are modelled as two transmission lines with the characteristic impedance Z_c, propagation constant β, and physical length l. All segments of the transmission lines are terminated the same matched load Z_c. The transmission line models of the electric and magnetic sources in the waveguide are given by the upper and lower subplots in Fig. 3(a).

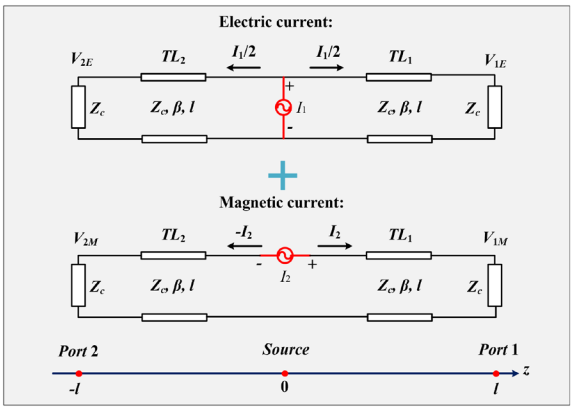

(a)

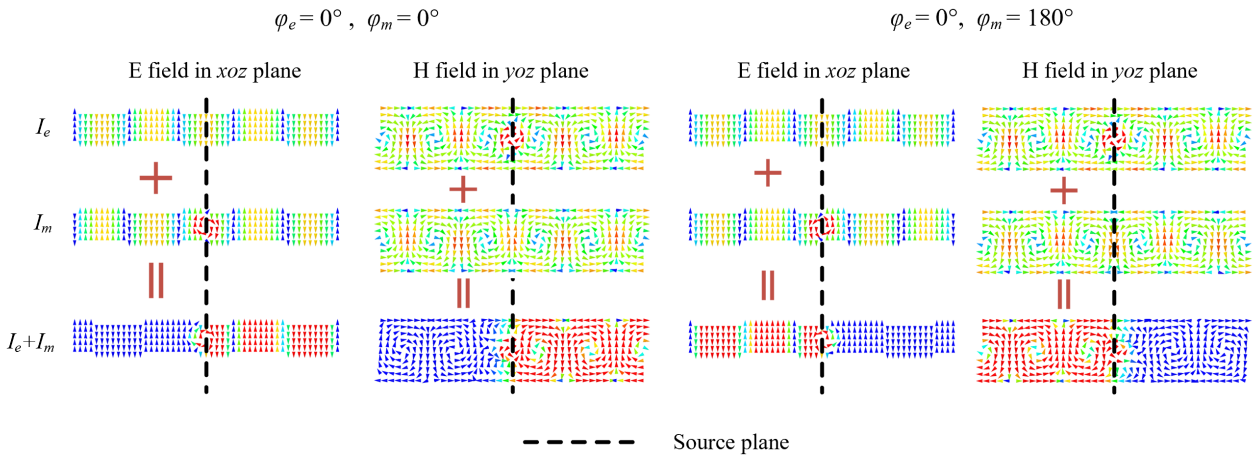

(b)

Fig. 3. (a) Transmission line model of the electric and magnetic dipoles located in the center of the rectangular waveguide. (b) The simulated electric field vectors (*xoz* plane) and magnetic field vectors (*yoz*) radiated by both dipoles individually and simultaneously in the waveguide at 10 GHz.

The ratio of the powers radiated in the $\pm z$ directions along their transmission lines is readily quantified when the shunt and series sources in Fig. 3(a) are excited with different relative phases. The currents associated with the electric and magnetic current models are given, respectively, by the relations:

$$I_{\omega}^{elec} = \frac{1}{2} I_1 e^{-j\beta z}\theta(z) + \frac{1}{2} I_1 e^{+j\beta z}\theta(-z) \tag{3}$$

$$I_{\omega}^{mag} = I_2 e^{-j\beta z}\theta(z) - I_2 e^{+j\beta z}\theta(-z) \tag{4}$$

where the electric current source in shunt, I_1, corresponds to the magnetic field discontinuity: $\vec{J}_s = \left[\hat{z}\times\left(\vec{H}_{>0} - \vec{H}_{<0}\right)\right]_{z=0}$ in the waveguide solution, and the magnetic current in series, I_2, corresponds to the electric field one: $\vec{K}_s = -\left[\hat{z}\times\left(\vec{E}_{>0} - \vec{E}_{<0}\right)\right]_{z=0}$. Therefore, the voltages corresponding to the electric fields at port 1 and port 2 in Fig. 1 are those at $z = +l$ and $z = -l$, respectively, in the transmission line models, i.e.,

$$V_{1E} = \frac{1}{2} I_1 e^{-j\beta l} \tag{5}$$

$$V_{2E} = \frac{1}{2} I_1 e^{-j\beta l} \tag{6}$$

$$V_{1M} = I_2 e^{-j\beta l} \tag{7}$$

$$V_{2M} = -I_2 e^{-j\beta l} \tag{8}$$

One clearly sees that if $I_1 = |I_1| e^{j\varphi_1}$ and $I_2 = |I_2| e^{j\varphi_2}$, then when the current sources are in-phase, i.e., when $\varphi_1 = \varphi_2$, and their magnitudes are balanced as $|I_1| = 2\,|I_2| = I_0$, then $V_{2E} + V_{2M} = 0$ and no power would be measured at port 2. On the other hand, $V_{1E} + V_{1M} = Z_c\, I_0$ at port 1 and all the power is measured there. Similarly, when they are out of phase, i.e., when $\varphi_1 - \varphi_2 = 180°$, then $V_{2E} + V_{2M} = Z_c I_0$ and $V_{1E} + V_{1M} = 0$. All the power is then measured at port 2 and zero is measured at port 1. The 3-D simulated field distributions associated with (1) and (2) corresponding to when the waveguide is individually excited by electric and magnetic sources on the plane at its center and by their combination are shown in Fig. 3(b). They confirm the transmission line results.

The average power flows along the $\pm z$-directions when the current magnitudes satisfy the balanced condition follow immediately from Eqs. (3)-(8). They are

$$P_{total}^{+z} = \frac{Z_c}{2} Re\left[\left(\frac{1}{2}I_1 + I_2\right)\left(\frac{1}{2}I_1 + I_2\right)^*\right] = \frac{1}{2} Z_c I_0^2 \left[1 + \cos(\varphi_1 - \varphi_2)\right] \tag{9}$$

$$P_{total}^{-z} = \frac{Z_c}{2} Re\left[\left(\frac{1}{2}I_1 - I_2\right)\left(\frac{1}{2}I_1 - I_2\right)^*\right] = \frac{1}{2} Z_c I_0^2 \left[1 - \cos(\varphi_1 - \varphi_2)\right] \tag{10}$$

Normalizing these average powers by $Z_c I_0^2$, the curves in Fig. 2 are obtained immediately. The peaks of those curves, of course, occur when $\varphi_1 - \varphi_2 = 0°$, i.e., $P_{total,norm}^{+z} = 1$, $P_{total,norm}^{-z} = 0$, and when $\varphi_1 - \varphi_2 = 180°$, i.e., $P_{total,norm}^{+z} = 0$, $P_{total,norm}^{-z} = 1$. Consequently, the transmission

line model indicates that once the source generates "vertical" (shunt) and "horizontal" (in-line) currents whose magnitudes are balanced, the ratio of the power flowing in both branches of the transmission system can be regulated by controlling the phase difference between those two currents. This design principle leads to the practical realization of the Huygens source in the actual waveguide system.

This example also illustrates that if the two currents have the proper balance of input powers, the amount of power flow in the antipodal directions is simply controlled by a phase difference between them. Thus, a practical realization only requires one tunable phase shifter, e.g., a commercial digital [37] or analog phase shifter [38]. Either element is easily integrated into the waveguide and, hence, either leads to a low-cost device. In contrast, conventional methods to achieve this type of multifunctional device would require two separate back-to-back waveguides, one 3-dB power divider, and two tunable attenuators. Thus, in comparison to the Huygens source approach, the conventional configuration is expensive, bulky and requires a complex integration process.

III. Experimental Results

An experiment was carried out to validate the theoretical results. A standard rectangular waveguide (WR-90) was fabricated with a circular hole in the bottom wall and with a slot in the top wall of the waveguide at its center. The 3-D simulation model and the prototype system are shown in Fig. 4. The center conductor of a SMA was extended through the bottom-wall hole into the waveguide to act as a vertical monopole as shown in Fig. 4(a). Taking into account its image in the bottom wall, the monopole acts as an electric dipole with its current moment I_e oriented vertically along the x-axis. A magnetic loop like the one reported in [39] was constructed for 10 GHz operation and was inserted through the top-wall slot as shown in Fig. 4(a). It acts as the magnetic dipole. Its orientation produces a horizontal current moment I_m along the y-axis [8]. The tail ends of the two excitations are offset by the same distance away from the yz-plane but on opposite sides of it. The detailed 3-D model presented in Fig. 4(a) was used to study the fields generated by the two sources in a comprehensive manner. Its physical dimensions are listed in Table I. The simulated electric and magnetic field vectors generated in the waveguide by both sources are individually shown in Fig. 5. The field distribution symmetries of the two excitations with respect to the center of the waveguide are apparent and in agreement with the idealized dipole source results shown in Fig. 3(b).

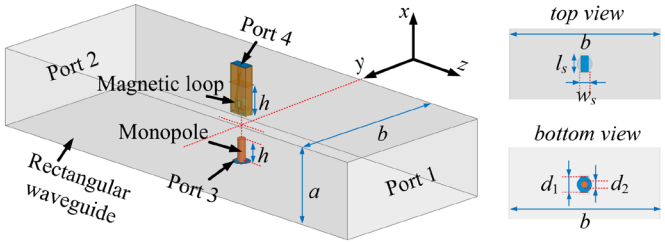

(a)

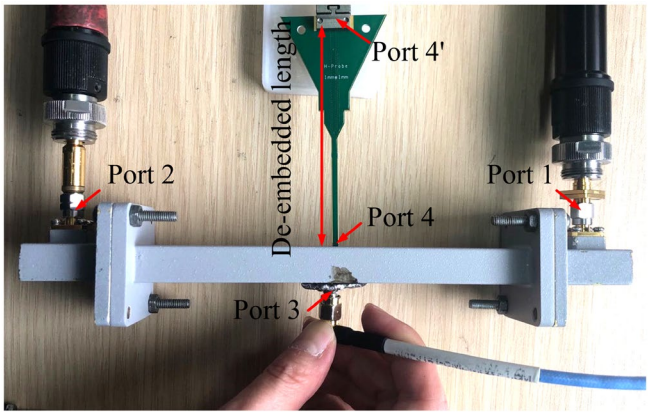

(b)

Fig. 4. The configuration of the waveguide experiment. (a) Simulation model. (b) The fabricated prototype under measurement conditions.

TABLE I
Physical Dimensions of the Waveguide Model (Unit: Millimeters)

a	b	h	l_s	w_s	d_1	d_2
10.16	22.86	3	3	1.5	2.3	1

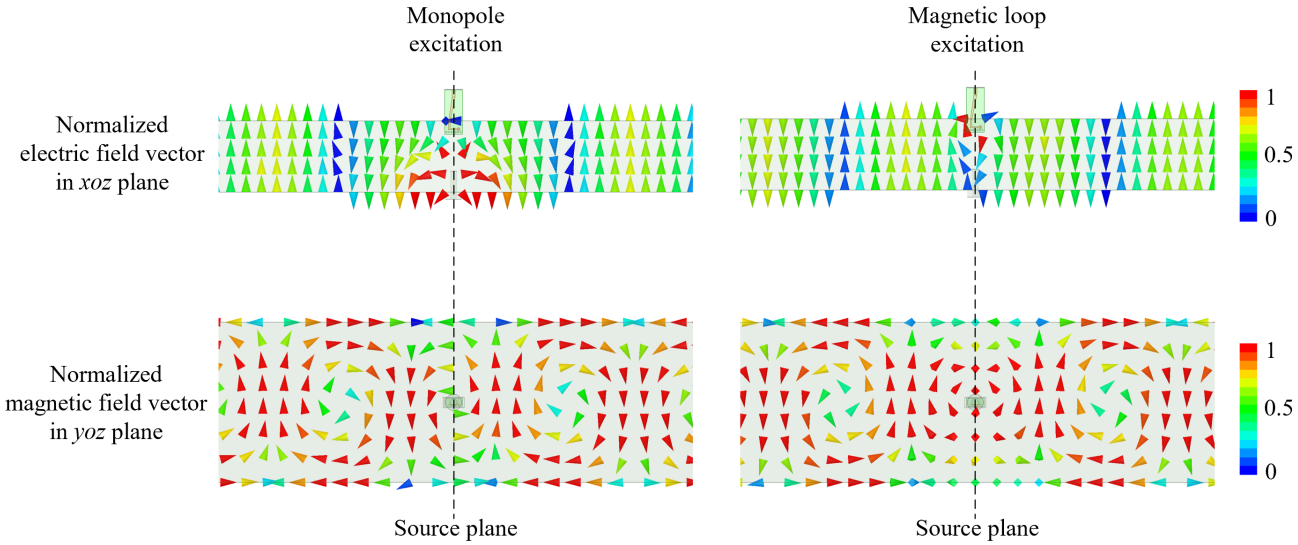

Fig. 5. Simulated electric and magnetic field vectors individually excited in the waveguide by the monopole and the magnetic loop at 10 GHz.

Two waveguide-to-coaxial converters are used to receive the power that flows in the two directions. Two ports are the feeds to the electric and magnetic dipoles. This four-port system is connected with a four-port Rohde & Schwarz ZVA67 vector network analyzer (VNA). The home-made magnetic loop was fabricated on a printed circuit board which has a length outside of the waveguide. Therefore, Port 4 in Fig. 4(b) is de-embedded to port 4' in order to obtain the *S* parameters with the correct reference phase. Furthermore, while both the monopole and loop are centered in the *xy*-plane at $z = 0$, their phase centers do not exactly coincide along the *x*-axis because their physical separation is necessary. This configuration is slightly different from those in the Huygens source antenna designs [16]-[26], as well as from the ideal dipole model in Fig. 1. Nevertheless, since this is an enclosed transmission line system, the power radiated by the dipoles propagates only along the *z*-axis. Consequently, the phase centers of both dipoles are exactly the same when referred to the *z*-axis; and the Huygens source behavior is attained.

Because they are a realistic monopole and magnetic loop, the magnitudes of the waveguide modes they generate are different from those obtained in the simulation model and are, of course, frequency-dependent. Thus, the fields they generate do not have the same amplitudes at different frequencies. As a result, the excitation voltages at port 3 and port 4 were adjusted to achieve the correct balance between them to attain the Huygens behavior. These voltages were finally fixed to be 1.0 V and 2.25 V, respectively, to reach the best balance at 10 GHz. These values generated the two currents, I_1 and I_2, shown in Fig. 3(a) with a balance equivalent to the analytical one: $|I_1| = 2\,|I_2| = I_0$. The phase difference between port 3 (φ_3) and port 4 (φ_4), $\Delta\varphi = \varphi_4 - \varphi_3$, was then varied. The measured results are shown in Fig. 6(a). When $\Delta\varphi = 0^\circ$, the power received at port 1 (P_1) was more than 10 dB larger than the power received at port 2 (P_2) in the range from 8.5−11.2 GHz. Conversely, when $\Delta\varphi = 180^\circ$, P_2 is more than 10 dB larger than P_1 in the range from 7.9 to 11.2 GHz. The measured power ratio, i.e., $|P_1\,(\text{dB}) - P_2\,(\text{dB})|$, of the unidirectional propagation in either case has a maximum magnitude of about 30 dB near 10 GHz. The frequency bands of the unidirectional power flow in these two cases cover most of the working frequency of the WR-90 waveguide (8.2−12.5 GHz). When $\Delta\varphi = 90^\circ$, P_1 and P_2 have nearly the same magnitude in the range from 9.2 to 11.3 GHz. The powers at the two ports were extracted and normalized at 10 GHz for different values of $\Delta\varphi$. These measured results are shown in Fig. 6(b). They are in excellent agreement with Fig. 2.

It is noted that this experiment did not focus on realizing a good match between the sources of the monopole and the loop when they were integrated into the waveguide. Thus, the voltage adjustments were necessary. Moreover, the powers at port 1 and port 2 were the values at their terminals and not the input powers of the sources for the monopole and the loop. They were attained by taking into account the reflection coefficients of those nonideal radiating elements. The excitation efficiency of the Huygens source in the waveguide transmission line system could be improved with several methods, for example, introducing loading dielectrics [40], using disc-ended structures [41] and L-loop structure [42]. These methods are being investigated as future work for designing practical products. Nonetheless, as a proof-of-concept experiment, our study successfully demonstrated that the Huygens source technique is able to regulate the flow of power in a microwave transmission line system over a wide band of frequencies.

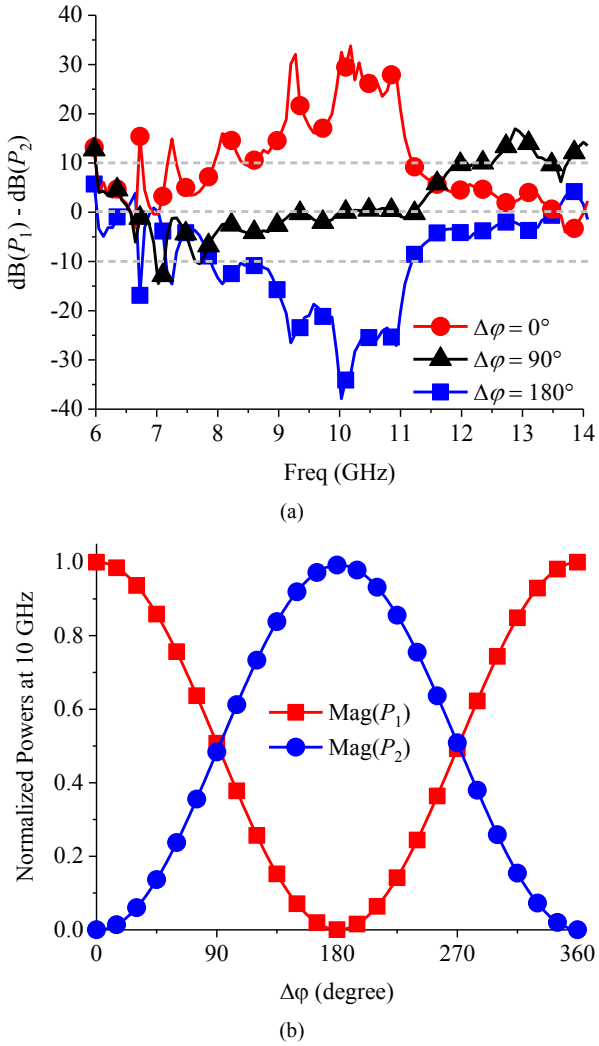

Fig. 6. (a) The ratio of the powers received at the two ports with respect to the source frequency. (b) The normalized powers received at the two ports at 10 GHz as functions of the phase difference between the electric and magnetic radiators.

IV. Conclusions

This work reported a Huygens source-based excitation technique to regulate the flow of power by controlling the state of the source in a microwave transmission line system, without introducing additional switches, structures, and materials in the signal's pathway. An equivalent transmission line model was developed to quantitatively predict its ability to regulate the flow of power along the transmission line in opposite directions. A proof-of-concept experiment validated the approach. The measured waveguide results, in very good agreement with their simulated values, demonstrated a large operational bandwidth with dynamic tunability of the power flows. The reported technique is quite suitable for application as a feed structure in innovative, miniaturized, and multifunctional RF systems.

REFERENCES

[1] X. Y. Zhang, J. Xu, and J. Chen, "High-power filtering switch with low loss and high isolation based on dielectric resonator," *IEEE Trans. Microw. Theory Techn.,* vol. 65, no. 6, pp. 2101-2110, Jun. 2017.

[2] H. Mizutani, R. Ishikawa, and K. Honjo, "InGaAs MMIC SPST switch based on HPF/LPF switching concept with periodic structure," *IEEE Trans. Microw. Theory Techn.,* vol. 64, no. 9, pp. 2863-2870, Sep. 2016.

[3] W. Fang, C. Chen, and Y. Lin, "2.4-GHz absorptive MMIC switch for switched beamformer application," *IEEE Trans. Microw. Theory Techn.,* vol. 65, no. 10, pp. 3950-3961, Oct. 2017.

[4] H. Boutayeb, P. R. Watson, W. Lu, and T. Wu, "Beam switching dual polarized antenna array with reconfigurable radial waveguide power dividers," *IEEE Trans. Antennas Propag.,* vol. 65, no. 4, pp. 1807-1814, Apr. 2017.

[5] Z. Tao, X. Wan, B. C. Pan, and T. J. Cui, "Reconfigurable conversions of reflection, transmission, and polarization states using active metasurface," *Appl. Phys. Lett.,* vol. 110, no. 12, 121901, Mar. 2017.

[6] L. Li *et al.*, "Electromagnetic reprogrammable coding-metasurface holograms," *Nat. Commun.,* vol. 8, no. 1, p. 197, Aug. 2017.

[7] M. R. LeRoy *et al.*, "High-speed reconfigurable circuits for multirate systems in SiGe HBT technology," *Proc. IEEE,* vol. 103, no. 7, pp. 1181-1196, Jul. 2015.

[8] D.M. Pozar, *Microwave Engineering*. 4th ed. New York, NY, USA: Wiley, 2011.

[9] F. Parment, A. Ghiotto, T. Vuong, J. Duchamp, and K. Wu, "Air-to-dielectric-filled two-hole substrate-integrated waveguide directional coupler," *IEEE Microw. Compon. Lett.,* vol. 27, no. 7, pp. 621-623, Jul. 2017.

[10] M. Zhang, J. Hirokawa, and M. Ando, "A four-way divider for partially-corporate feed in an alternating-phase fed single-layer slotted waveguide array," *IEEE Trans. Antennas Propag.,* vol. 56, no. 6, pp. 1790-1794, Jun. 2008.

[11] J. Cai, X. Wu, and J. Feng, "A cosine-shaped vane-folded waveguide and ridge waveguide coupler," *IEEE Trans. Electron Devices,* vol. 63, no. 6, pp. 2544-2549, Jun. 2016.

[12] D. Zarifi, A. Farahbakhsh, A. U. Zaman, and P. Kildal, "Design and fabrication of a high-gain 60-GHz corrugated slot antenna array with ridge gap waveguide distribution layer," *IEEE Trans. Antennas Propag.,* vol. 64, no. 7, pp. 2905-2913, Jul. 2016.

[13] A. Pourzadi, A. R. Attari, and M. S. Majedi, "A directivity-enhanced directional coupler using epsilon negative transmission line," *IEEE Trans. Microw. Theory Techn.,* vol. 60, no. 11, pp. 3395-3402, Nov. 2012.

[14] J. Shi, J. Qiang, K. Xu, and J. Chen, "A balanced branch-line coupler with arbitrary power division ratio," *IEEE Trans. Microw. Theory Techn.,* vol. 65, no. 1, pp. 78-85, Jan. 2017.

[15] B. K. O. Neil and J. L. Young, "Experimental investigation of a self-biased microstrip circulator," *IEEE Trans. Microw. Theory Techn.,* vol. 57, no. 7, pp. 1669-1674, Jul. 2009.

[16] W. Love, "Some highlights in reflector antenna development," *Radio Sci.,* vol. 11, no. 8-9, pp. 671-684, Aug.-Sep.1976.

[17] S. R. Best, "Progress in the design and realization of an electrically small Huygens source," in *2010 International Workshop on Antenna Technology (iWAT)*, pp. 1-4, 2010.

[18] P. Jin and R. W. Ziolkowski, "Metamaterial-inspired, electrically small, Huygens sources," *IEEE Antennas Wireless Propag. Lett.*, vol. 9, pp. 501-505, May 2010.

[19] R. W. Ziolkowski, P. Jin, and C. Lin, "Metamaterial-inspired engineering of antennas," *Proc. IEEE,* vol. 99, no. 10, pp. 1720-1731, Oct. 2011.

[20] R. W. Ziolkowski, "Low profile, broadside radiating, electrically small Huygens source antennas," *IEEE Access,* vol. 3, pp. 2644-2651, Dec. 2015.

[21] M.-C. Tang, H. Wang, and R. W. Ziolkowski, "Design and testing of simple, electrically small, low-profile, Huygens source antennas with broadside radiation performance," *IEEE Trans. Antennas Propag.,* vol. 64, no. 11, pp. 4607-4617, Nov. 2016.

[22] M.-C. Tang, T. Shi, and R. W. Ziolkowski, "Electrically small, broadside radiating Huygens source antenna augmented with internal non-Foster elements to increase its bandwidth," *IEEE Antennas Wireless Propag. Lett.,* vol. 16, pp. 712-715, 2017.

[23] M.-C. Tang, B. Zhou, and R. W. Ziolkowski, "Low-profile, electrically small, Huygens source antenna with pattern-reconfigurability that covers the entire azimuthal plane," *IEEE Trans. Antennas Propag.,* vol. 65, no. 3, pp. 1063-1072, Mar. Apr. 2017.

[24] W. Lin and R. W. Ziolkowski, "Electrically-small, low-profile, Huygens circularly polarized antenna," *IEEE Trans. Antennas Propag.*, vol. 66, no. 2, pp. 636-643, Feb. 2018.

[25] M.-C. Tang, Z. Wu, T. Shi, and R. W. Ziolkowski, "Electrically small, low-profile, planar, Huygens dipole antenna with quad-polarization diversity," *IEEE Trans. Antennas Propag.,* vol. 66, no. 12, pp. 6772-6780, Dec. 2018.

[26] S. Lee, G. Shin, S. M. Radha, J. Choi, and I. Yoon, "Low-profile, electrically Small planar Huygens source antenna with an endfire radiation characteristic," *IEEE Antennas Wirel. Propag. Lett.,* vol. 18, no. 3, pp. 412-416, Mar. 2019.

[27] F. J. Rodríguez-Fortuño, G. Marino, P. Ginzburg, D. O'Connor, A. Martínez, G. A. Wurtz, and A. V. Zayats, "Near-field interference for the unidirectional excitation of electromagnetic guided modes," *Science,* vol. 340, no. 6130, pp. 328-30, Apr. 2013.

[28] R. W. Ziolkowski, "Huygens multipole arrays to realize unidirectional needle-like radiation," *Phys. Rev. X*, vol. 7, 031017, Jul. 2017.

[29] I. Liberal, I. Ederra, R. Gonzalo, and R. W. Ziolkowski, "Induction theorem analysis of resonant nanoparticles: Design of a Huygens source nanoparticle laser," *Phys. Rev. Applied*, vol. 1, 044002, May 2014.

[30] T. Van Mechelen and Z. Jacob, "Universal spin-momentum locking of evanescent waves," *Optica,* vol. 3, pp. 118-126, Jan. 2016.

[31] L. Marrucci, "Spin gives direction," *Nat. Phys.,* vol. 11, pp. 9-10, Dec. 2014.

[32] M. F. Picardi, A. V. Zayats, and F. J. Rodriguez-Fortuno, "Janus and Huygens dipoles: Near-field directionality beyond spin-momentum locking," *Phys. Rev. Lett.,* vol. 120, no. 11, 117402, Mar. 2018.

[33] D. J. Bisharat and D. F. Sievenpiper, "Guiding waves along an infinitesimal line between impedance surfaces," *Phys. Rev. Lett.,* vol. 119, no. 10, 106802, Sep. 2017.

[34] A. Taflove, *Computational Electrodynamics: The Finite-Difference Time- Domain Method*. Boston, MA, USA: Artech House, 1995.

[35] D. E. Merewether, R. Fisher, and F. W. Smith, "On implementing a numeric Huygen's source scheme in a finite difference program to illuminate scattering bodies," *IEEE Trans. Nucl. Sci.*, vol. 27, no. 6, pp. 1829-1833, Dec. 1980.

[36] T. Martin and L. Pettersson, "Dispersion compensation for Huygens' sources and far-zone transformation in FDTD," *IEEE Trans. Antennas Propag.*, vol. 48, no. 4, pp. 494-501, Apr. 2000.

[37] F. Ellinger, R. Vogt, and W. Bachtold, "Ultracompact reflective-type phase shifter MMIC at C-band with 360º phase-control range for smart antenna combining," *IEEE J. Solid-State Circuits,* vol. 37, no. 4, pp. 481-486, Apr. 2002.

[38] F. Ellinger, H. Jackel, and W. Bachtold, "Varactor-loaded transmission-line phase shifter at C-band using lumped elements," *IEEE Trans. Microw. Theory Techn.,* vol. 51, no. 4, pp. 1135-1140, Apr. 2003.

[39] R. Yang, X. Wei, Y. Shu, and Y. Yang, "A high-frequency and high spatial resolution probe design for EMI prediction," *IEEE Trans. Instrum. Meas.,* vol. 68, no. 8, pp. 3012-3019, Aug. 2019.

[40] M. E. Bialkowski, "Analysis of a coaxial-to-waveguide adaptor incorporating a dielectric coated probe," *IEEE Microw. Guided Wave Lett.,* vol. 1, no. 8, pp. 211-214, Aug. 1991.

[41] M. E. Bialkowski, "Analysis of a coaxial-to-waveguide adaptor including a discended probe and a tuning post," *IEEE Trans. Microw. Theory Techn.,* vol. 43, no. 2, pp. 344-349, Feb. 1995.

[42] H. Ma, B. Liang, Y. Shi, and J. Miao, "Analysis of coaxial-to-waveguide transitions in end launcher type," in *Proc. 2012 International Conference on Microwave and Millimeter Wave Technology (ICMMT)*, Shenzhen, China, vol. 3, pp. 1-4, 2012.